Ionics (2013) 19:391–394
DOI 10.1007/s11581-012-0766-0

ORIGINAL PAPER

A new anode material $LiZnVO_4$: synthesis and electrochemical measurements

Yunyan Lin · Fuyu Xiao · Shaokang Gao

Received: 4 February 2012 / Revised: 29 May 2012 / Accepted: 21 June 2012 / Published online: 24 July 2012

Abstract $LiZnVO_4$ particles ware synthesized via solid-state reaction route. It was characterized by X-ray diffraction and scanning electron microscopy. As anode material for rechargeable lithium-ion battery, the electrochemical performance of the $LiZnVO_4$ samples was measured. It was found that a large capacity of 330 mAh g^{-1} can be retained after 70 cycles. The electrochemical measurements indicate that the anode material made of $LiZnVO_4$ exhibits excellent cycling stability even at a high current density.

Keywords Anode material · $LiZnVO_4$ · Electrochemical properties · Lithium-ion battery

Introduction

Lithium-ion batteries (LIBs) are being intensively pursued for hybrid electric vehicle and plug-in hybrid electric vehicle applications. Nowadays, most of the commercial LIBs use graphite as anode material for its excellent cycling behavior. However, low theoretical capacity and poor cycling behavior for graphite anode at a high current density limit its large-scale application in high energy-density battery systems. Thus, much attention has been paid to develop new anode materials [1–3]. Recently, the vanadates have generated a new interest shown to be potential candidates for anode material in LIBs [4–9]. For instance, brannerite structural MnV_2O_6 and inverse spinel structural $LiNiVO_4$ can react with a large number of lithium ions per formula unit at a low voltage [10, 11]. Although these vanadate compounds have large initial capacity, they would become amorphous after the first cycle and exhibited a large capacity loss upon the subsequent cycles [4, 12]. So far, several methods have been developed to enhance their electrochemical properties. MnV_2O_6 synthesized by a hydrothermal route can deliver a reversible capacity of 630 mAh g^{-1} after 30 cycles [13]. Amorphous $LiNiVO_4$ thin films obtained by the physical vapor deposition technique exhibited discharge capacity of 800–1,100 mAh g^{-1} after 20 cycles [14]. According to a report by Denis et al. [12, 15], during the electrochemical reduction of these vanadates, oxygen acts as a redox center of Li–O bonds thereby leading to an enhancement in capacity. Accordingly, it can be stated that the 2*p* orbital of oxygen may play an important role for the compensation of charge equivalence besides transition metals during the insertion and extraction of Li ion.

In the present work, we synthesized $LiZnVO_4$ via a solid-state reaction route and used it as anode material in a rechargeable lithium-ion battery. The electrochemical measurements indicated that the cells made of $LiZnVO_4$ exhibited a large capacity and excellent cycling stability.

Experimental

Synthesis of $LiZnVO_4$

$LiZnVO_4$ was synthesized by a solid-state reaction. In a typical process, lithium carbonate (Li_2CO_3), zinc oxide (ZnO), and vanadium pentoxide (V_2O_5) were ground in an agate mortar at a Li/Zn/V=1:1:1. The mixture was sintered at 750 °C for 3 h. X-ray diffraction (XRD) patterns were recorded on a PANalytical X′Pert spectrometer using CoKα radiation (λ=1.78897 Å), and the data were converted to CuKα data. Scanning electron microscopy (SEM) and transmission electron microscopy (TEM) images were taken on a Philips-XL30 instrument and a JEOL 2010 instrument, respectively.

Y. Lin · F. Xiao · S. Gao (✉)
College of Chemistry and Chemical Engineering,
Fuzhou University,
Fuzhou, Fujian 350002, China
e-mail: gaosk@fzu.edu.cn

Electrochemical measurements

The electrochemical behaviors of the materials were examined via CR2025 coin-type cells with lithium metal as the counter electrode. The anode materials were made by mixing active materials, acetylene black and PVDF, in a weight ratio of 60:30:10, respectively. The electrolyte was 1 M $LiPF_6$ in a 1:1:1 (volume ratio) mixture of ethylene carbonate, ethylene methyl carbonate, and dimethyl carbonate. The separator was a UP 3093 (Japan) microporous polypropylene membrane. Cell assembly was carried out in a glove box under an argon atmosphere. The discharge and charge tests for aqueous lithium-ion battery were carried out by a program-controlled Battery Test System (Land CT 2001A, Wuhan, China) at different constant current density with a cutoff voltage of 0.02–2.5 V. All the electrochemical measurements were performed at room temperature.

Results and discussion

Figure 1 shows the crystal structure of $LiZnVO_4$. It contains three types of tetrahedra, [VO_4] and two disordered mixed-site [Li/ZnO_4] tetrahedral. The ratio of lithium and zinc in the mixed-site [Li/ZnO_4] tetrahedra is 1:1, and the hexagonal channels are along the [0001] direction [16].

The XRD pattern of the product synthesized at 750 °C for 3 h is shown in Fig. 2a. All the diffraction reflections can be indexed to a rhombohedra structure $LiZnVO_4$ (JCPDS 38-1332). According to JCPDS 38-1332, $LiZnVO_4$ belongs to the rhombohedra crystal system with space group R-3h. The unit cell volume is 1,653.49 $Å^3$, and the lattice parameters are $a=b=14.1857$ Å, $c=9.4877$ Å, $\alpha=\beta=90°$, $\gamma=120°$, $Z=18$ [17]. Figure 2b shows the SEM image of $LiZnVO_4$ synthesized at 750 °C for 3 h. It clearly shows that the product is composed of irregular particles, and their size is found to be several micrometers.

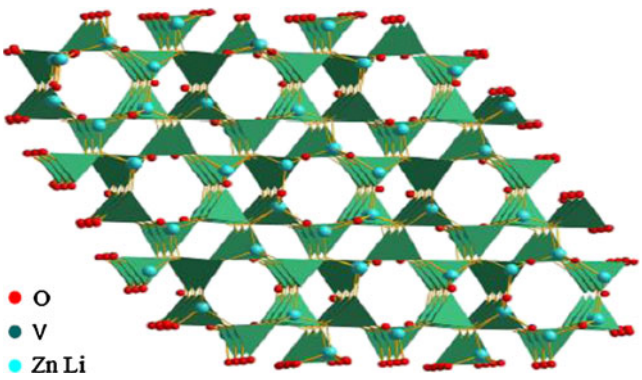

Fig. 1 Crystal structure of $LiZnVO_4$

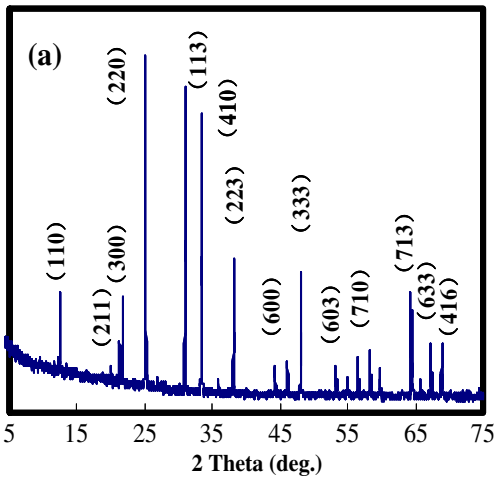

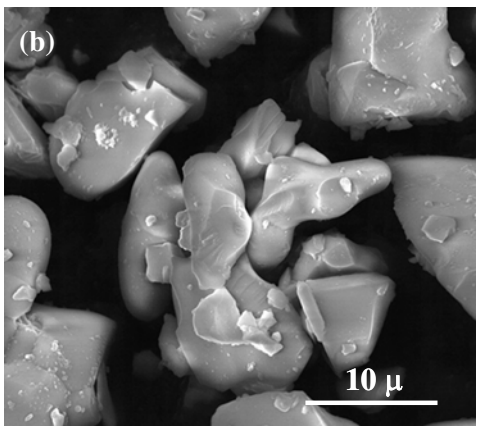

Fig. 2 XRD pattern (**a**) and SEM image (**b**) of $LiZnVO_4$ synthesized at 750 °C

The electrochemical properties of $LiZnVO_4$ have been investigated, and the results are shown in Fig. 3. Figure 3a shows cyclic voltammetry (CV) curves of the cells made of $LiZnVO_4$ at a scan rate of 0.5 mV s^{-1}. As can be seen from Fig. 3a, the CV curves between the first cycle and the following cycles are different. This result might be attributed to the fact that the irreversible structured transformation has been taking place in the initial cycle. After the first cycle, the CV curves changed slightly, indicating that the lithium ions' intercalation/deintercalation into/out of the $LiZnVO_4$ electrode is well reversible. Figure 3b shows the charge–discharge profiles of anodes made of $LiZnVO_4$ particles at the 1st, 2nd, 20th, 50th, and 70th cycles recorded at a current density of 1 A g^{-1}, and a larger irreversible discharge capacity of 824 mAh g^{-1} was observed. This might be attributed to the structure transformation to amorphous at the initial cycle [13, 18]. It can be found from Fig. 3c that the capacity tends to decrease in the initial cycling period, then stopped decreasing, and eventually reached a plateau, indicating that the electrochemical properties of $LiZnVO_4$ anode are very stable, and the Li-ion intercalation/deintercalation into/out of

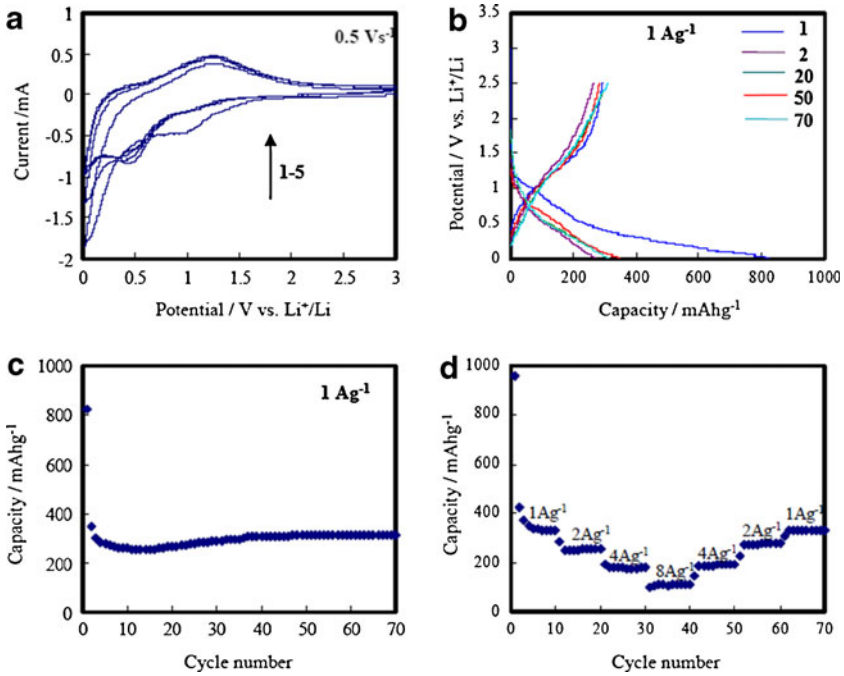

Fig. 3 CV curves (**a**), charge–discharge profiles (**b**), and cycling performances of $LiZnVO_4$ anode at different current densities(**c**, **d**)

the electrode is well reversible even at a current density of 1 Ag^{-1}. A reversible capacity of ca. 330 mAh g^{-1} was obtained after 70 cycles corresponding to x=2.3 for Li_xZnVO_4. Even after the current density was increased to 8 Ag^{-1}, a reversible capacity of 110 mAh g^{-1} was also achieved (see Fig. 3d). On the other hand, the capacity can be recovered, and the cycling stability can be retained after the current density was increased significantly. This might be attributed to the intrinsic characteristics of anode. As mentioned above, the hexagonal channels along the [0001] direction in the crystal structure could provide a diffusion space for Li-ion intercalation/deintercalation into/out of the anode, resulting in very good cycling stability. Meanwhile, the amorphous structure of $LiZnVO_4$ might improve the capacity for creating a smoother pathway during the Li-ion insertion and extraction process. A similar result was also observed for the NaV_6O_{15} electrode [19].

To further research the electrochemical reaction mechanism of $LiZnVO_4$, XRD and TEM were measured on the anode recovered from the cells at selected voltages. Figure 4a shows the XRD patterns of the anode after discharge and charge. The peaks indicated by solid triangle symbols are attributed to Li_2CO_3, which most likely results from the reaction of Li_2O and CO_2 in air, and Li_2O might come from the electrochemical process of discharge and charge. The similar result was also observed by Orsini and coworkers [4]. As shown in the TEM image, only the Li_2CO_3 phase is observed, while the crystalline $LiZnVO_4$ cannot be detected, indicating that it was transferred into amorphous phase at the first cycle, which is in agreement with CV measurement.

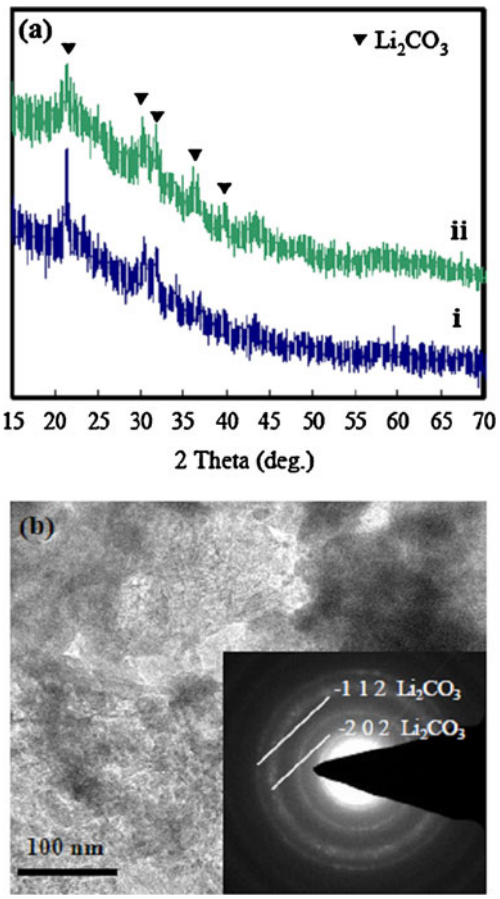

Fig. 4 **a** XRD patterns of the cell made of $LiZnVO_4$ (*i* discharged to 0.02 V and *ii* charged to 2.5 V, respectively) and **b** TEM image of the anode discharged to 0.02 V at the first cycle

Conclusions

In summary, $LiZnVO_4$ has been synthesized via a solid-state reaction route and then was used as anode material in a rechargeable Li-ion battery. A large capacity of 330 mAh g^{-1} was retained after 70 cycles even at a current density of 1 A g^{-1}. The electrochemical measurements indicate that the anode material made of $LiZnVO_4$ particles displayed excellent cycling stability. This might be attributed to the intrinsic characteristics of anode material. These results might renew interest in the design of anode material in the future.

Acknowledgments This work was financially supported by grants from the Natural Science Foundation of Fujian Province (2011J033).

References

1. Zhang WM, Wu XL, Hu JS, Guo YG, Wan LJ (2008) Adv Funct Mater 18:3941–3946
2. Kim MG, Cho J (2009) Adv Funct Mater 19:1497–1514
3. Yang R, Huang J, Zhao W, Lai WZ, Zhang XZ, Zheng J, Li XG (2010) J Power Sources 195:6811–6816
4. Orsini F, Baudrin E, Denis S, Dupont L, Touboul M, Guyomard D, Piffard Y, Tarascon J-M (1998) Solid State Ionics 107:123–133
5. Denis S, Baudrin E, Orsini F, Ouvrard G, Touboul M, Tarascon J-M (1999) J Power Sources 81–82:79–84
6. Guyomard D, Sigala C, Le Gal La Salle A, Piffard Y (1997) J Power Sources 68:692–697
7. Ram M (2011) Int J Mod Phys B 25(12):1619–1628
8. Prakash D, Masuda Y, Sanjeeviraja C (2012) Ionics 18(1–2):31–37
9. Clemens O, Bauer M, Haberkorn R, Beck HP (2011) Z Anorg Allg Chem 637(7–8):1036–1044
10. Kim SS, Ikuta H, Wakihara M (2001) Solid State Ionics 139:57–65
11. Han XY, Tang WC, Yi ZH, Sun JT (2008) J Appl Electrochem 38:1671–1676
12. Hara D, Shirakawa J, Ikuta H, Uchimoto Y, Wakihara M, Miyanagab T, Watanabe I (2002) J Mater Chem 12:3717–3722
13. Huang WD, Gao SK, Ding XK, Jiang LL, Wei MD (2010) J Alloys Compd 495:185–188
14. Reddy MV, Pecquenard B, Vinatier P, Levasseur A (2007) Surf Interface Anal 39:653–659
15. Denis S, Baudrin E, Touboul M, Tarascon J-M (1997) J Electrochem Soc 144:4009–4109
16. Azrour M, Elouadi B, Ammari LE (2010) Acta Cryst E 66:i39
17. Capsoni D, Bini M, Massarotti V, Mustarelli P, Belotti F, Galinetto P (2006) J Phys Chem B 110(11):5409–5415
18. Rossignol C, Ouvrard G, Baudrin E (2001) J Electrochem Soc 148:869–877
19. Liu HM, Wang YG, Li L, Wang KX, Hosonoa E, Zhou HS (2009) J Mater Chem 19:7885–7891